Singh, Ugrasen; Tirkkonen, Olav

Robust Link Adaptation in Multiantenna URLLC Systems with Flashlight Interference

Published in:
IEEE Communications Letters

DOI:
10.1109/LCOMM.2024.3451018

Published: 01/01/2024

Robust Link Adaptation in Multiantenna URLLC Systems With Flashlight Interference

Ugrasen Singh, *Member, IEEE*, and Olav Tirkkonen, *Fellow, IEEE*

***Abstract*— We present a robust link-adaptation method to realize ultra-reliable and low-latency communications (URLLC) against *flashlight*, i.e., on-off interference. A robust link-adaptation method is presented based on the measured signal-to-interference plus noise ratio (SINR) at the URLLC user, which varies between the time when interference power is measured and the time of payload transmission. We obtain the statistical distribution of the change of SINRs between two consecutive time slots and devise backoff methods guaranteeing the reliability of transmissions against flashlight interference. We derive the average transmission rate over Rayleigh fading channels in the considered system model. We observe that in the presence of flashlight interference, a strict reliability requirement reduces the transmission rate to a small fraction of the best effort service rate. When increasing the number of antennas at both the serving and interfering transmitters, the increase in array gain is partially compromised by the increased backoff needed to guarantee reliability. All analytical results are verified via Monte Carlo simulation.**

***Index Terms*— Backoff, beamforming, link-adaptation, outage capacity, precoder, Rayleigh fading, URLLC.**

I. Introduction

ULTRA-RELIABLE and low-latency communication (URLLC) plays a vital role in machine-type 5G wireless networks [1]. In mobile broadband (MBB) services, reliability is guaranteed by employing radio link control protocols such as automatic repeat request (ARQ) and hybrid-ARQ (HARQ) [2]. These protocols allow the retransmission of lost packets to guarantee reliability, which incurs high latency. In latency-critical URLLC use cases, e.g., in industrial automation, packet delays are, however, strictly limited [3], or retransmission of lost packets is not allowed, but a new packet is needed within a strict survival time limit [4].

Robust link adaptation for downlink URLLC has been considered in [5], [6], [7], [8], and [9]. In [5], the combined effect of changes in wanted signal quality and interference power arising from user mobility, as well as changes in multiantenna beamforming at interferers was considered. Robustness was achieved by applying a backoff to the measured signal-to-interference-and-noise ratio (SINR) values, based on quantiles of the SINR distribution. As the number of interferers increases, the overall interference power may increase, but the need for backoff decreases, indicating that the reliability of the communication system improves [5]. In [6] and [7], a single-cell single antenna system is considered, where devices report channel quality indicators (CQI) in terms of quantized signal-to-noise ratio (SNR) values to the serving base station (BS). Further, [8], [9] consider a wideband multicellular multiantenna system, with several subbands in the frequency domain. In [8], robustness against changes in channel quality and interference is achieved by reporting a CQI that provides a target error performance on the M worst subchannels. However, this work lacks modeling for the optimal choice of M worst channels that are sufficient enough to tackle the channel burst in subsequent transmissions in the presence of flashlight interference. Open loop link adaptation (OLLA) methods are considered in [9], where the BS adapts the transmission method based on reported CQI. The reliability and latency performance of OLLA is compromised by acknowledgment errors. Link-adaptation for guaranteeing reliability against interference in a distributed multiple-input multiple-output (MIMO) system is discussed in [10]. This letter concentrates on developing joint transmission strategies to improve robustness.

Flashlight interference [11], arising in cellular systems due to uncoordinated beamforming at BSs, compromises CQI predictability. While multi-antenna transmit beamforming is perceived to improve the predictability of wireless communications due to the channel hardening effect [12], it simultaneously makes the flashlight effect worse. Interference perceived by a victim receiver varies in an unpredictable manner subject to beamforming decisions of interfering cells. In the simulation-driven approaches of [8] and [9], the considered robust link adaptation methods are capable of adapting themselves to the varying multiantenna interference in the channels. However, due to the lack of comprehensive analytical modeling, the sensitivity of performance to system parameters remains elusive.

In this letter, we address the effect of flashlight interference on downlink URLLC services in a multicellular multiple-input single-output (MISO) system with uncoordinated beamforming. We concentrate on the situation where the only uncertainty related to the channel quality of the URLLC user comes from the flashlight effect, in the worst case when all interference at the user comes from one BS.

We analyze URLLC performance in closed form, assuming that the interfering BS selects the precoder based on its own served user, thus changing it at random from the perspective of the URLLC user. The results show that even in a scenario where the only uncertainty is the flashlight effect, guaranteeing reliability reduces the achievable transmission rate to a small fraction of what one would expect for best effort traffic. While increasing the number of transmit antennas leads to array gain and an improvement of the wanted signal, our results

Manuscript received 4 June 2024; revised 12 July 2024 and 21 August 2024; accepted 25 August 2024. Date of publication 28 August 2024; date of current version 11 October 2024. This work was funded in part by Business Finland under the project "Extreme Machine Type Communications for 6G" and by the Research Council of Finland (grant 345109). The associate editor coordinating the review of this letter and approving it for publication was A. Nasir. *(Corresponding author: Ugrasen Singh.)*

The authors are with the Department of Information and Communications Engineering, Aalto University, 110016 Helsinki, Finland (e-mail: ugrasen.singh@aalto.fi; olav.tirkkonen@aalto.fi).

Digital Object Identifier 10.1109/LCOMM.2024.3451018

concretely show how simultaneously the predictability of the interference reduces, thus compromising part of the array gain in a URLLC setting. The main contributions of this work are: 1) We compute the statistical distribution of changes in SINR between two consecutive time slots, caused by flashlight interference. 2) We derive the statistical distribution of the measured SINR and use it to obtain the average transmission rate for URLLC service against flashlight interference.

II. System Model and Link-Adaptation

We consider a MISO system depicted in Fig. 1, where a BS provides downlink URLLC service to a user which suffers from the interference of a neighboring BS. Each BS serves a number of users, and at each time slot, the BS schedules a user to be served in the allocated set of resources. We assume that the BSs have N_t transmit antennas. We consider the situation where all interference comes from one source, and the user has a single antenna. Conditioned on an average interference power, this is the worst-case scenario of flashlight interference in the context of URLLC. If the interfering BS would spatially multiplex multiple users in each time slot, the interference distribution would be more benign at the victim—the interference would be spread to a wider angular range, resulting in a lower level of flashlight interference happening more often. In the limit of the interferer multiplexing N_t users with no power control, interference variability would vanish.

For simplicity, we assume that the channels are quasi-static. The effects of time-selective fading can be analyzed using the methods of [5]. We concentrate on a frequency flat setting poor of diversity, relevant in, e.g., an indoor factory scenario with wide coherence bandwidth. Also, multiantenna beamforming will asymptotically lead to a frequency-flat channel due to channel hardening. We also assume that the BS performs perfect maximum ratio transmission (MRT) based on perfect knowledge of the wanted CSI, and that CQI feedback from the user to the BS is perfect. In 5G, CSI at BS can be acquired by channel reciprocity, or high-precision Type-II feedback [13]. Effects of CSI estimation errors and feedback quantization on URLLC can be addressed following, e.g., [14].

The BS transmits pilot symbols to the user, allowing the user to measure the SINR. We assume that the user has an estimate of the statistics of the interference. Based on the measured instantaneous SINR, and the statistics, the user computes a CQI in the form of a recommended transmission rate and feeds it back to the serving BS.

We consider a scenario where the interfering BS serves a group of users, and schedules transmissions to different users in different time slots. For this, the interfering BS selects the precoding vector according to the CSI of its scheduled user, without coordinating with the BS serving the user of interest. This leads to an ON/OFF -type flashlight effect at the interference victim user.

The channel gain vector from the serving BS to the user is $\mathbf{h} = [h_1, h_2, \ldots ..h_{N_t}]^{\mathrm{T}} \in \mathcal{C}^{N_t \times 1}$ and the vector from the interfering BS to the user is $\mathbf{g} = [g_1, g_2, \ldots ..g_{N_t}]^{\mathrm{T}} \in \mathcal{C}^{N_t \times 1}$. The elements of $\mathbf{h}$ and $\mathbf{g}$ are modeled as complex Gaussian distributed with zero mean and unity variance. The presented analysis can be extended to any channel distribution, albeit with added complexity.

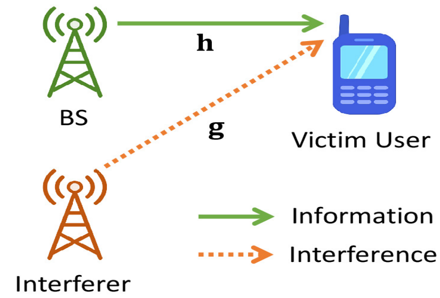

Fig. 1. Illustration of MISO system for URLLC transmission.

Link-adaptation is based on the measurement performed at the user during the pilot transmission. As we are considering a cellular system with multiuser scheduling, the interferer transmits to a different user at the time of measurement than during the URLLC transmission of interest. At time $t = 0$, the serving BS transmits pilot symbols s_0 with precoding vector $\mathbf{w} \in \mathcal{C}^{N_t \times 1}$ to the user. The received equivalent baseband signal is given by

$$y_0 = \mathbf{h}^{\mathrm{T}} \mathbf{w} s_0 + \mathbf{g}^{\mathrm{T}} \mathbf{v}_0 x_0 + n_0, \tag{1}$$

where the subscript denotes the time, $\mathbb{E}\left[|\, s_0\,|^2\right] = p_{\mathrm{W}}$, $\mathbb{E}\left[|\, x_0\,|^2\right] = p_{\mathrm{I}}$, n_0 is additive white Gaussian noise (AWGN) with zero mean and variance N_0, and $\mathbf{v}_0 \in \mathcal{C}^{N_t \times 1}$ is the unitary precoding vector adopted by the interfering BS during the time of measurement, and x_0 is the corresponding transmitted symbol. The MRT precoding vector for the user of interest is $\mathbf{w} = \mathbf{h}^* / \|\mathbf{h}\|$.

Due to the flashlight effect, the SINR measured at $t = 0$ is not the same as the SINR during the payload transmission—another precoder may be used at the interference source. The received signal at time τ of payload transmission becomes

$$y_\tau = \mathbf{h}^{\mathrm{T}} \mathbf{w} s_\tau + \mathbf{g}^{\mathrm{T}} \mathbf{v}_\tau x_\tau + n_\tau, \tag{2}$$

where $\mathbf{v}_\tau \in \mathcal{C}^{N_t \times 1}$ is the unitary precoding vector used by the interferer at time of payload transmission, and $\mathbb{E}\left[|\, s_\tau\,|^2\right] = p_{\mathrm{W}}, \mathbb{E}\left[|\, x_\tau\,|^2\right] = p_{\mathrm{I}}$. The unitary precoders $\mathbf{v}_0$ and $\mathbf{v}_\tau$ are chosen by the interferer from N_t-dimensional space based on the channels of users it serves. From the p.o.w. of the interference victim, these are random precoders, we model them as selected uniformly from the space of all MISO precoders.

Due to changes in interferer precoding, the received interference power at the victim user may change over consecutive time slots. With Γ_0 the SINR estimated at $t = 0$, the objective is to select a transmission mode such that the probability of failure of payload transmission is smaller than a P_{out}, characterizing the URLLC service. This outage probability may be fixed for the service, or it may be adaptively selected based on a survival strategy [4]. From (1), using perfect MRT, the SINR at the victim receiver at time $t = 0$ becomes

$$\Gamma_0 = \frac{p_{\mathrm{W}} |\mathbf{h}|^2}{p_{\mathrm{I}} |\mathbf{g}\mathbf{v}_0|^2 + N_0} = \frac{\hat{\gamma}\, |\mathbf{h}|^2}{\tilde{\gamma}\, |\mathbf{g}\mathbf{v}_0|^2 + 1}, \tag{3}$$

where $\hat{\gamma} = \frac{p_{\mathrm{W}}}{N_0}$ and $\tilde{\gamma} = \frac{p_{\mathrm{I}}}{N_0}$ denote transmit SNRs. Similarly, the received SINR for the payload transmission (2) is

$$\Gamma_\tau = \frac{\hat{\gamma}\, |\mathbf{h}|^2}{\tilde{\gamma}\, |\mathbf{g}\mathbf{v}_\tau|^2 + 1}\,. \tag{4}$$

Let us assume that the SINR Γ_τ at the time of payload transmission fully characterizes reception success. Knowing Γ_0, the flashlight effect can be overcome by selecting an appropriate backoff θ for robust link-adaptation such that

$$\Pr\left(\Gamma_\tau < \frac{\Gamma_0}{\theta}\right) \leq P_{\text{out}}\,. \tag{5}$$

For the AWGN channel, a tight bound for the achievable transmission rate for finite block code length is derived in [15, Theorem 54]. Since we assume that all channels are Gaussian and quasi-static frequency-flat fading, for sufficiently large block code length, a tight approximation for the maximum achievable rate is given by [16, Eq. (4)]:

$$R \approx C(P_{\text{out}}) + \mathcal{O}\left(\frac{\log_2(l)}{l}\right), \tag{6}$$

where $C(P_{\text{out}}) = (1-P_{\text{out}})\log_2\left(1+\frac{\Gamma_0}{\theta}\right)$ denotes the outage capacity of the channel, and the Bachmann-Landau asymptotics $\mathcal{O}(\cdot)$ can be approximated by half of its argument. Since θ only depends on the uncertainty of the interference, it does not depend on $\mathbf{h}$, it only depends on P_{out} and the relative interference statistics.

III. Performance Analysis

A. Backoff Analysis

To counter the effects of flashlight interference on SINR at the user, we evaluate the robust link-adaption backoff to guarantee URLLC service for the transmission of interest. We first compute the ratio of SINRs at time $t=0$ and $t=\tau$:

$$Z = \frac{\Gamma_\tau}{\Gamma_0} = \frac{Y}{X}, \tag{7}$$

where $Y = \tilde{\gamma}\,|\mathbf{g}\mathbf{v}_0|^2 + 1$ and $X = \tilde{\gamma}\,|\mathbf{g}\mathbf{v}_\tau|^2 + 1$. The power of the interfering channel is $\alpha = \|\mathbf{g}\|^2$.

Certain properties of the cumulative distribution function (CDF) $F_Z(z)$ follow directly from Z being a ratio of two i.i.d. random variables (RVs). We have $\mathrm{P}_r(Y \leq Xz) = \mathrm{P}_r(X \leq Yz)$ from which it follows that $\mathrm{P}_r(X/Y \geq 1/z) = \mathrm{P}_r(X/Y \leq z)$. Thus $F_Z(z) = F_{1/Z}(z)$. This directly yields

$$F_Z(z) = 1 - F_Z\left(\frac{1}{z}\right) \quad \text{and} \quad f(z) = \frac{1}{z^2} f\left(\frac{1}{z}\right). \tag{8}$$

It is thus sufficient to know $F_Z(z)$ for either $z<1$ or for $z>1$, and we always have $F_Z(1) = \frac{1}{2}$.

The statistics of interference power can be derived from spherical cap analysis on the complex sphere with radius α. Based on [14], interference power is distributed as

$$F_Y(y) = 1 - \left(k - \frac{y}{\lambda}\right)^{N_t-1}, \quad 1 \leq y \leq \lambda+1\,, \tag{9}$$

with the corresponding probability density function (PDF) $f_Y(y) = \left(\frac{N_t-1}{\lambda}\right)\left(k-\frac{y}{\lambda}\right)^{N_t-2}$, where $\lambda = \alpha\tilde{\gamma}$ and $k = 1+\frac{1}{\lambda}$. The random variable X is distributed similarly.

To obtain the required backoff for ensuring URLLC to the user of interest, we need $F_Z(z)$. Let us first derive the PDF of the inverse of interference power $V = \frac{1}{X}$. Its CDF is:

$$F_V(v) = 1 - F_X\left(\frac{1}{v}\right) = \left(k - \frac{1}{\lambda v}\right)^{N_t-1}, \; \frac{1}{\lambda+1} \leq v \leq 1\,. \tag{10}$$

After taking the derivative of (10) w.r.t. v, the PDF of V is

$$f_V(v) = \left(\frac{N_t-1}{\lambda v^2}\right)\left(k - \frac{1}{\lambda v}\right)^{N_t-2}, \; \frac{1}{\lambda+1} \leq v \leq 1\,. \tag{11}$$

Now, the ratio of SINRs can be written as $Z = YV$, and the CDF of Z can be obtained as

$$F_Z(z) = \int_{\frac{1}{\lambda+1}}^{z} f_Z(z)\,dz, \quad \frac{1}{\lambda+1} \leq z \leq \lambda+1\,, \tag{12}$$

where $f_Z(z)$ denotes the PDF of RV z. The PDF $f_Z(z)$ can be obtained with the help of [17], it is given by

$$f_Z(z) = \int_1^{z(\lambda+1)} f_V\left(\frac{z}{y}\right) f_Y(y)\frac{1}{y}dy, \quad \frac{1}{\lambda+1} \leq z \leq 1\,, \tag{13}$$

while for $z>1$ it can be obtained from (8).

By substituting $f_Y(y)$ from (9) and (11) into (13) and performing a binomial expansion, $f_Z(z)$ can be expressed as

$$f_Z(z) = \sum_{m,n=0}^{N_t-2} \frac{c_{mn}}{z^{n+2}} \int_1^{z(\lambda+1)} y^{m+n+1}dy, \tag{14}$$

where

$$c_{mn} = (N_t-1)^2\binom{N_t-2}{m}\binom{N_t-2}{n}(-1)^{m+n} \frac{k^{2N_t-4-m-n}}{\lambda^{m+n+2}}.$$

After solving the integral in (14), $f_Z(z)$ is given by

$$f_Z(z) = \sum_{m,n=0}^{N_t-2} \frac{c_{mn}}{m+n+2}\left((1+\lambda)^{m+n+2}z^m - \frac{1}{z^{n+2}}\right). \tag{15}$$

By substituting (15) into (12), we get the CDF

$$F_Z(z) = \sum_{m,n=0}^{N_t-2} \frac{c_{mn}}{m+n+2}\int_{\frac{1}{\lambda+1}}^{z} \left((1+\lambda)^{m+n+2}z^m - \frac{1}{z^{n+2}}\right)dz, \tag{16}$$

where $\frac{1}{\lambda+1} \leq z \leq 1$. After solving the integral in (16), and algebraic computations, the CDF of Z in the range $\frac{1}{\lambda+1} \leq z \leq 1$ becomes:

$$\begin{aligned} F_Z(z) =& \sum_{m,n=0}^{N_t-2} \frac{c_{mn}(\lambda+1)^{m+n+2}}{(m+1)(m+n+2)}\left(z^{m+1} - (\lambda+1)^{-m-1}\right) \\ &+ \sum_{m,n=0}^{N_t-2} \frac{c_{mn}}{(n+1)(m+n+2)}\left(z^{-n-1} - (\lambda+1)^{n+1}\right) \\ =& \,\Gamma(N_t)\sum_{m=0}^{N_t-2} e_m\left((\lambda+1)^{m+1}z^{m+1} - 1\right) \\ &+ \frac{(\lambda+1)^{2N_t-4}}{\lambda^{2N_t-2}}\sum_{n=0}^{N_t-2} d_n\left(z^{-n-1} - (\lambda+1)^{n+1}\right), \end{aligned} \tag{17}$$

where

$$e_m = \binom{N_t-2}{m}(N_t-1)(-1)^m \frac{(\lambda+1)^{2N_t-m-3}\Gamma(m+1)}{\lambda^{2N_t-2}\Gamma(N_t+m+1)}$$

$$d_n = \binom{N_t-2}{n}\frac{(-1)^n(N_t-1)^2}{(n+1)(n+2)(\lambda+1)^n}\,{}_2F_1\left[n+2, 2-N_t, n+3, \frac{1}{1+\lambda}\right]$$

and $\Gamma(\cdot)$ denotes the upper complete gamma function. $F_Z(z)$ for $1 \leq z \leq \lambda+1$ can be directly obtained by using (8). This expression of the CDF can be used for deriving the backoff.

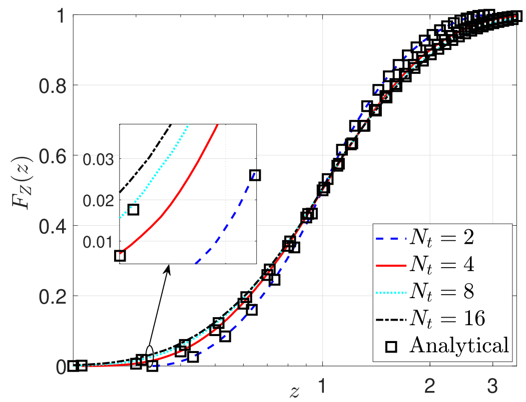

Fig. 2. CDF of ratio of SINRs for different values of N_t.

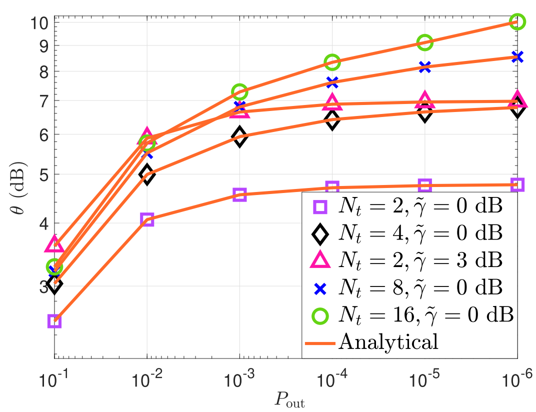

Fig. 3. Backoff versus P_{out} plots for various values of N_t and $\hat\gamma = 0$ dB.

From (5) and (17), we get:

$$\theta = \frac{1}{F_Z^{-1}(P_{\text{out}})}. \tag{18}$$

B. Outage Capacity Analysis

The outage capacity is defined as the maximum data rate that can be achieved given a specified outage probability, i.e., the probability that the information is not decoded successfully. The outage capacity depends on both the outage probability and SINR. If the SINR during transmission were precisely known, we could directly choose an optimal capacity reaching transmission rate, with zero outage probability. In presence of a measured SINR Γ_0, and SINR uncertainty, we have to select a backoff. From (6), the outage capacity can be Jensen upper bounded as

$$C(P_{\text{out}}) \leq (1 - P_{\text{out}}) \log_2\left(1 + \frac{\bar\Gamma_0}{\theta}\right), \tag{19}$$

where $\bar\Gamma_0$ is the average measured SINR. To evaluate $\bar\Gamma_0$, we need to model the PDF of SINR Γ_0. From (3), RV $U = \hat\gamma|\mathbf{h}|^2$ is central Chi-square distributed with mean $\frac{\hat\gamma}{2}$ and $2N_t$ degrees of freedom [18]. The PDF of RV U is given by

$$f_U(u) = \frac{u^{N_t-1}}{(\hat\gamma)^{N_t}\Gamma(N_t)}\exp\left(\frac{-u}{\hat\gamma}\right), \quad u > 0, \tag{20}$$

where $\Gamma(\cdot)$ denotes the upper complete gamma function. Now, SINR can be written as $\Gamma_0 = \frac{U}{Y}$.

Proposition 1: The PDF of Γ_0 is as follows:

$$f_{\Gamma_0}(r) = \beta_{mn}\left(\frac{r^{n-1}}{\hat\gamma^n}\exp\left(\frac{-r}{\hat\gamma}\right) + \left(\Gamma\left(m+n+1, \frac{r}{\hat\gamma}\right) - \Gamma\left(m+n+1, \frac{r(\lambda+1)}{\hat\gamma}\right)\right) \cdot \frac{(m+1)\hat\gamma^{m+1}}{r^{m+2}} - (\lambda+1)^{m+n+1}\exp\left(\frac{-r(\lambda+1)}{\hat\gamma}\right)\frac{r^{n-1}}{\hat\gamma^n}\right),$$
$$r > 0 \tag{21}$$

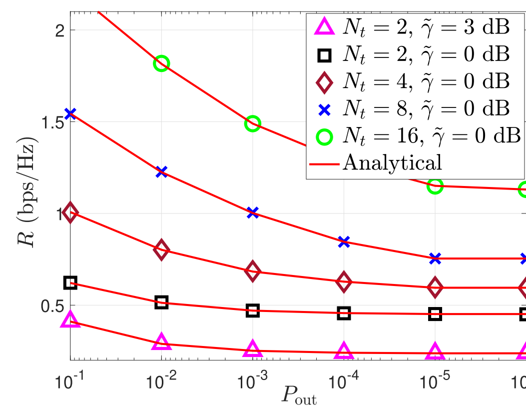

Fig. 4. Transmission rate versus P_{out} plots for different number of N_t.

where $\Gamma(\cdot,\cdot)$ denotes the upper incomplete gamma function and $\beta_{mn} = (N_t - 1)\sum_{m=0}^{N_t-2}\sum_{n=0}^{N_t-1}\binom{N_t-2}{m}k^{N_t-m-2}\frac{(-1)^m}{\lambda^{m+1}n!}$.

Proof: See Appendix A ■

The average SINR $\bar\Gamma_0$ can be obtained as $\bar\Gamma_0 = \int_\epsilon^\infty r f_{\Gamma_0}(r), \quad \epsilon \to 0$. By substituting $f_{\Gamma_0}(r)$ into $\bar\Gamma_0$ and solving the integral, $\bar\Gamma_0$ can be expressed as

$$\bar\Gamma_0 = \beta_{mn}\left(\hat\gamma\Gamma\left(n+1, \frac{\epsilon}{\hat\gamma}\right) + (m+1)(m+n)!\hat\gamma \sum_{l=0}^{m+n}\left(\frac{\Gamma\left(l-m, \frac{\epsilon}{\hat\gamma}\right)}{l!} - \frac{(\lambda+1)^m\Gamma\left(l-m, \frac{(\lambda+1)\epsilon}{\hat\gamma}\right)}{(l!)^2}\right) - \hat\gamma(\lambda+1)^m \Gamma\left(n+1, \frac{\epsilon(\lambda+1)}{\hat\gamma}\right)\right). \tag{22}$$

Finally, by substituting this into (19), we will have the average outage capacity.

IV. Numerical Results

In this section, we present numerical results and discuss how uncoordinated beamforming at the interferer can affect the performance of a URLLC user. We assume that the total transmit power from the BSs is the same in the measurement and payload transmission times, while the serving BS adapts the transmission rate according to obtained backoff values. We consider a block code of length $l = 200$.

Fig. 2 illustrates the CDF plots for the ratio of SINRs for $\tilde\gamma = \hat\gamma = 0$ dB, and different values of N_t. We can observe from the figure that the tail probabilities of the interference ratio increase with increasing N_t, indicating that interference power varies frequently between the time of measurement and payload transmission. As a result, the CDF of SINR at the time of transmission has larger variance when N_t increases.

With increasing N_t at the interfering BS, the number of interference degrees of freedom increases, which results in increased uncertainty of the flashlight effect at the victim user.

Backoff versus P_{out} plots are depicted in Fig. 3 for different values of N_t and $\tilde{\gamma}$. It can be observed from the figure that the required backoffs increase with increasing N_t. Also, for a fixed number of antennas (here $N_t = 2$), the required backoff increases when interference SINR $\tilde{\gamma}$ increases. Backoff plots become flat for very small values of P_{out}, as according to (17), the tail of the interference power ratio is limited to $\frac{1}{1+\lambda}$, i.e., $Z \geq \frac{1}{1+\lambda}$. Thus, the required backoff increases with increasing N_t at the interfering BS and $\tilde{\gamma}$.

Fig. 4 demonstrates the transmission rate versus P_{out} plots for different values of $N_t, \tilde{\gamma}$, and $\hat{\gamma} = 0$. We can see from the figure that the transmission rate increases with the number of antennas at the BSs for a given P_{out} due to array gain from beamforming at the serving BS. However, for a fixed N_t, the transmission rate reduces with decreasing P_{out}. It is important to note that for low P_{out}, uncoordinated beamforming at the interfering BS deprives the victim user of part of gain from beamforming at the serving BS. From the perspective of URLLC, having a huge number of antennae at the BSs is not hardening the channels, rather it is softening them. Thus, the flashlight effect reduces the impact of the BS antenna array gain at the user. Finally, as expected, for a fixed number of antennas (here $N_t = 2$), the URLLC transmission rate reduces when $\tilde{\gamma}$ increases.

V. Conclusion

We have analyzed the the effect of flashlight interference on URLLC services in the presence of an interferer employing beamforming, where the user served by the interferer changes between the time that the URLLC user measures the quality of its channel, and the time of the data transmission towards the URLLC user. We have observed that the uncertainty of the interference increases with an increasing number of transmit antennas at the BSs. The achievable URLLC transmission rate is thus compromised by the increasing number of transmit antennas at interferer; part of the array gain of the wanted signal power is reduced by the flashlight effect of interference.

Appendix A

From (3), $\Gamma_0 = \frac{U}{Y}$, the CDF of Γ_0 can be expressed as

$$F_{\Gamma_0}(r) = \mathrm{P_r}\left(\Gamma_0 \leq r\right) = \int_1^{\lambda+1}\int_0^{ry} f_U(u) f_Y(y) du\, dy. \quad (23)$$

By substituting (15) and (9) into (23) and after solving the inner integral, $F_{\Gamma_0}(r)$ can be written as

$$F_{\Gamma_0}(r) = \frac{N_t - 1}{\lambda\,\Gamma(N_t)} \int_1^{\lambda+1} \gamma\left(N_t, \frac{ry}{\hat{\gamma}}\right)\left(k - \frac{y}{\lambda}\right)^{N_t - 2} dy. \quad (24)$$

Binomially expanding (24) and writing the lower incomplete gamma function as an upper gamma function, we get

$$F_{\Gamma_0}(r) = q_m \int_1^{\lambda+1} y^m \left(\Gamma(N_t) - \Gamma\left(N_t, \frac{ry}{\hat{\gamma}}\right)\right) dy, \quad (25)$$

where $q_m = \frac{N_t - 1}{\lambda^{m+1}\,\Gamma(N_t)} \sum_{m=0}^{N_t-2} \binom{N_t-2}{m} k^{N_t - m - 2}(-1)^m$. By using $\Gamma(n,x) = (n-1)!\exp(-x)\sum_{l=0}^{n-1}\frac{x^l}{l!}$ and solving the integral, $F_{\Gamma_0}(r)$ can be expressed as

$$\begin{aligned} F_{\Gamma_0}(r) = {} & \frac{q_m \Gamma(N_t)}{m+1}\left((1+\lambda)^{m+1} - 1\right) \\ & - q_m (N_t - 1)! \sum_{n=0}^{N_t-1}\left(\frac{\hat{\gamma}}{r}\right)^{m+1} \\ & \cdot \frac{1}{n!}\left(\Gamma\left(m+n+1, \frac{r}{\hat{\gamma}}\right)\right. \\ & \left. - \Gamma\left(m+n+1, \frac{r(\lambda+1)}{\hat{\gamma}}\right)\right). \quad (26) \end{aligned}$$

The PDF of Γ_0 can be obtained by differentiating, leading to $f_{\Gamma_0}(r)$ in Proposition 1.

References

[1] K. S. Kim et al., "Ultrareliable and low-latency communication techniques for tactile internet services," *Proc. IEEE*, vol. 107, no. 2, pp. 376–393, Feb. 2019.

[2] E. Dahlman, S. Parkvall, and J. Sköld, *4G: LTE/LTE-Advanced for Mobile Broadband*. Amsterdam, The Netherlands: Elsevier, 2011.

[3] P. Popovski et al., "Wireless access in ultra-reliable low-latency communication (URLLC)," *IEEE Trans. Commun.*, vol. 67, no. 8, pp. 5783–5801, Aug. 2019.

[4] S. R. Khosravirad et al., "Communications survival strategies for industrial wireless control," *IEEE Netw.*, vol. 36, no. 2, pp. 66–72, Mar. 2022.

[5] U. Oruthota, F. Ahmed, and O. Tirkkonen, "Ultra-reliable link adaptation for downlink MISO transmission in 5G cellular networks," *Information*, vol. 7, no. 1, p. 14, Mar. 2016.

[6] A. Belogaev, E. Khorov, A. Krasilov, D. Shmelkin, and S. Tang, "Conservative link adaptation for ultra reliable low latency communications," in *Proc. IEEE Int. Black Sea Conf. Commun. Netw. (BlackSeaCom)*, Jun. 2019, pp. 1–5.

[7] S. Praveen, J. Khan, and L. Jacob, "Reinforcement learning based link adaptation in 5G URLLC," in *Proc. 8th Int. Conf. Smart Comput. Commun. (ICSCC)*, Jul. 2021, pp. 159–163.

[8] G. Pocovi, A. A. Esswie, and K. I. Pedersen, "Channel quality feedback enhancements for accurate URLLC link adaptation in 5G systems," in *Proc. IEEE 91st Veh. Technol. Conf. (VTC-Spring)*, May 2020, pp. 1–6.

[9] E. Peralta, G. Pocovi, L. Kuru, K. Jayasinghe, and M. Valkama, "Outer loop link adaptation enhancements for ultra reliable low latency communications in 5G," in *Proc. IEEE 95th Veh. Technol. Conf. (VTC-Spring)*, Jun. 2022, pp. 1–7.

[10] M. Alonzo, P. Baracca, S. R. Khosravirad, and S. Buzzi, "URLLC for factory automation: An extensive throughput-reliability analysis of D-MIMO," in *Proc. 24th Int. ITG Workshop Smart Antennas*, Feb. 2020, pp. 1–6.

[11] A. Osseiran and A. Logothetis, "Closed loop transmit diversity in WCDMA HS-DSCH," in *Proc. IEEE 61st Veh. Technol. Conf.*, vol. 1, Jun. 2005, pp. 349–353.

[12] B. M. Hochwald, T. L. Marzetta, and V. Tarokh, "Multiple-antenna channel hardening and its implications for rate feedback and scheduling," *IEEE Trans. Inf. Theory*, vol. 50, no. 9, pp. 1893–1909, Sep. 2004.

[13] *5G; NR; Physical Layer Procedures for Data*, document TS 38.214, Version 16.2.0, 3GPP, 2020.

[14] K. K. Mukkavilli, A. Sabharwal, E. Erkip, and B. Aazhang, "On beamforming with finite rate feedback in multiple-antenna systems," *IEEE Trans. Inf. Theory*, vol. 49, no. 10, pp. 2562–2579, Oct. 2003.

[15] Y. Polyanskiy, H. V. Poor, and S. Verdu, "Channel coding rate in the finite blocklength regime," *IEEE Trans. Inf. Theory*, vol. 56, no. 5, pp. 2307–2359, May 2010.

[16] W. Yang, G. Durisi, T. Koch, and Y. Polyanskiy, "Quasi-static multiple-antenna fading channels at finite blocklength," *IEEE Trans. Inf. Theory*, vol. 60, no. 7, pp. 4232–4265, Jul. 2014.

[17] A. G. Glen, L. M. Leemis, and J. H. Drew, "Computing the distribution of the product of two continuous random variable," *Comput. Statist. Data Anal.*, vol. 44, no. 3, pp. 451–464, 2004.

[18] M. K. Simon, *Probability Distributions Involving Gaussian Random Variables: A Handbook for Engineers and Scientists*. Berlin, Germany: Springer, 2006.